Available online at www.sciencedirect.com
ScienceDirect
Journal of Photochemistry and Photobiology A: Chemistry 187 (2007) 152–159
Journal of Photochemistry and Photobiology A:Chemistry
www.elsevier.com/locate/jphotochem

Investigations on the adsorption behavior of Neutral Red on mercaptoethane sulfonate protected gold nanoparticles

Li Shang, Xiangqin Zou, Xiue Jiang, Guocheng Yang, Shaojun Dong *

State Key Laboratory of Electroanalytical Chemistry, Changchun Institute of Applied Chemistry, Chinese Academy of Sciences, Graduate School of the Chinese Academy of Sciences, Changchun, Jilin 130022, People's Republic of China

Received 17 April 2006; received in revised form 15 July 2006; accepted 12 October 2006
Available online 29 October 2006

Abstract

A detailed investigation on the adsorption behavior of Neutral Red (NR) molecules on mercaptoethane sulfonate-monolayer protected gold clusters (MES-MPCs) has been conducted by the spectroscopic method. It is found that cationic NR molecules are adsorbed on the negatively charged MPCs surfaces via electrostatic attractive forces. The absorption study shows that the optical properties of NR molecules are significantly influenced upon the adsorption. Based on the electrostatic adsorption nature and the excellent stability of MES-MPCs against the electrolytes, this association can be released by the addition of electrolyte salts, which can be monitored by both absorption and fluorescence spectroscopy. In addition, dication Ca^{2+} is found to be more effective in the release of NR than univalent Na^{+}. Moreover, the MES-MPCs exert energy transfer quenching of NR fluorescence by both static and dynamic quenching. However, static quenching seems to be the dominating quenching mechanism. Furthermore, this energy transfer quenching exhibits strong dependence of Au core size, and 5.0 nm MPCs show stronger ability in quenching the NR fluorescence than that of 2.7 nm MPCs.

Keywords: Neutral Red; Monolayer protected gold clusters; Adsorption; Spectroscopy

1. Introduction

In recent years, nanostructured materials are gaining a wide attention in nanotechnology, since materials in nanometer size regime display widely interesting size-dependent optical, electronic and chemical properties [1–5]. Of particular interest are the organic–inorganic nanohybrid assemblies that have potential applications in developing nanodevices and biosensors [6,7]. Modification of the nanocluster surfaces with photoactive molecules can enhance the photochemical activity, and render the organic–inorganic nanohybrid materials suitable for sensors and optoelectronic applications [8]. The key to create such nanocomposite materials is to understand surface interactions at the molecular level and develop strategies of refining properties of nanoparticle superstructures. To date, most of these studies are limited to semiconductor nanocluster systems, and considerable interest has been shown to modify the surface of semiconductor colloids with sensitizers and redox couples [9–12]. For example, capping them with organic dyes and other semiconductors are found to alter the photophysical and photocatalytic properties of semiconductor colloids [13–15]. Besides semiconductor nanoclusters, basic understanding of the interaction between metal nanoparticles and photoactive molecules such as dyes is also important for developing organic–inorganic nanohybrid assemblies [7,16,17].

Several recent investigations have focused on understanding the nature of those interactions between dye molecules and metal nanoparticles. Chen and Chang have investigated the assembly of Nile Red onto citrate-protected gold nanoparticles, and found a highly fluorescent product forming on the surface of gold nanoparticles [18]. Ghosh et al. have studied the emission behavior of 1-methylaminopyrene upon adsorbing to the gold nanoparticles. They described a straightforward experimental verification of the size effect of metal nanoparticles on fluorescence quenching of a molecular probe [19]. Ding et al. have studied the adsorption characteristics of thionine on gold nanoparticle surfaces by means of various analytical techniques. Their studies showed that the addition of gold nanoparticles resulted in an obvious aggregation of thionine [20]. However, most of these studies are performed just on the commonly

* Corresponding author. Fax: +86 431 5689711.
E-mail address: dongsj@ns.ciac.jl.cn (S. Dong).

1010-6030/$ – see front matter © 2006 Elsevier B.V. All rights reserved.
doi:10.1016/j.jphotochem.2006.10.008

prepared colloids like citrate-protected metal nanoparticles, and scarce attention has been paid to the adsorption of photoactive molecules on thiolate ligands protected metal clusters which are known as monolayer-protected clusters (MPCs) [21–23]. In fact, MPCs are of particular research interest in developing nanoassemblies for applications in material science, biological science and chemical platforms [22,24–26]. This mainly because the metal core is coated with a relatively dense monolayer of thiolate ligands, which gives rise to much better stability than that of commonly prepared colloids like citrate-protected metal nanoparticles. On the other hand, since the collective surface area of the MPCs in a solution can be quite large, a substantial sensitivity may be possible relative to the binding interactions traditionally conducted on flat surfaces [27]. Therefore, modification of such MPCs with photoactive molecules offers exciting opportunities for the design of novel photon-based devices for sensing, switching, and drug delivery [7,24]. In spite of these potential advantages, scarce research has been reported on studying the adsorption behaviour of dye molecules on MPCs, which is of great importance in broadening their applications [28–30]. In one recent work of our group [31], we described the synthesis of water-soluble gold nanoparticles encapsulated by mercaptoethane sulfonate by the way of one-phase method. Here, in this paper, we present our efforts in understanding the adsorption behaviour of dye molecule–Neutral Red (NR) on mercaptoethane sulfonate-monolayer protected gold clusters (MES-MPCs). NR is known as a representative phenazine dye, which has been used in studies of biological systems, especially as an intracellular pH indicator [32,33], a non-toxic stain [34,35], and a probe material [36–38]. In this article, the adsorption behavior of NR on MES-MPCs was investigated in detail by UV–vis adsorption spectroscopy and fluorescence spectroscopy. The nature of the adsorption, the mechanism of fluorescence quenching of adsorbed NR, the size dependent quenching effect were investigated. We also presented a quasi-reversible nanoparticles/photoactive molecules binding equilibrium in this contribution.

2. Experimental

2.1. Materials

Mercaptoethanesulfonic sodium salt (98%) was purchased from Aldrich, sodium borohydride (98%) was purchased from ACROS, $HAlCl_4$ was purchased from Beijing Chemical Company, Neutral Red was bought from Shanghai No.1 Chemical Company, and used after recrystallization from ethanol. All other reagents were of analytical reagent grade, and used as received. The water used was purified through a Millipore system.

2.2. Synthesis of MES-MPCs

The MES-MPCs were synthesized by a modification of reported procedure [31]. Briefly, a freshly prepared 0.4 M sodium borohydride aqueous solution ($NaBH_4/Au = 10$) was added quickly into a 50 mL aqueous solution of $HAlCl_4$ (1 mM) and mercaptoethane sulfonate (1 mM) with vigorous stirring. After further stirred for 1 h, the reaction was terminated. Finally the solution was dialyzed before their use for further studies. The MPCs with a larger core size were prepared by the same procedure except that the mole ratio of thiol to $AuCl_4^-$ of 0.1:1 was used in the reaction. The nanoparticles core sizes are moderately polydisperse, and the average core diameter is 2.7 ± 0.5 nm and 5.0 ± 1.0 nm, respectively, which was determined by TEM analysis. The MPCs employed in our experiment were the smaller one (2.7 nm) unless otherwise stated.

2.3. Spectroscopic measurements

UV–vis absorption spectra were recorded with a Cary 500 UV–vis-NIR spectrometer (Varian), fluorescence measurements were performed on a LS-55 Luminescence Spectrometer (Perkin-Elmer). The emission spectra were recorded in the wavelength of 570–800 nm upon excitation at 540 nm and 460 nm at pH 6.0 and 7.8, respectively, using 10 nm/10 nm slit widths. The experiments were performed by keeping the concentration of NR constant while varying the concentration of MPCs. This was done by mixing an appropriate amount of NR solution and various proportions of MPCs solution, while maintaining the total volume of the solution constant. All test solutions were incubated for 15 min before the spectra were obtained to ensure complete adsorption. Moreover, the mixture of NR and MPCs solutions prepared in our experiment was quite stable, and no sign of aggregation was found within 1 week of storage. A 1.00 cm path length rectangular quartz cell was used for these measurements. No buffer was employed in these experiments, and the pH of the NR aqueous solution (pH 6.0) did not show any perceptible changes in the presence of MPCs or electrolytes. The experiments were repeated and found to be reproducible within experimental errors. All the experiments were performed at room temperature (293 K).

3. Results and discussion

3.1. Absorption characteristic of NR solution

As known, NR has pH dependent structural equilibrium between the protonated form (acid form) and alkanolamine form (neutral form) with a pK_a 6.8 [39]. In aqueous solution, the absorption spectrum of NR shows maximum absorption centered around 530 nm at low pH (e.g. 6.0) and 465 nm at high pH (e.g. 7.8), corresponding to the acid form and neutral form respectively [40,41]. Fig. 1 shows the structural equilibrium of NR. As shown, NR is similar to other planar dyes in the chemical structures belonging to the acridine, thiazine, and xanthene groups, and the acid form of NR is positively charged. A distinctive color change from yellow to red as NR is protonated from the basic form can be observed.

3.2. Adsorption of NR on MES-MPCs

Fig. 2 shows the absorption spectra of 5×10^{-6} M NR containing various concentrations of MPCs. As shown in

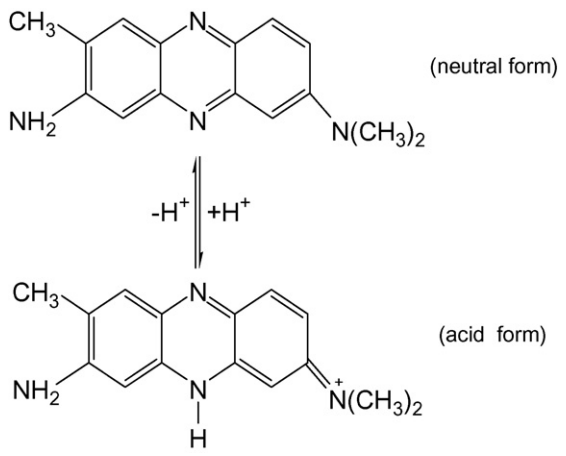

Fig. 1. Structural equilibrium of Neutral Red in aqueous solution.

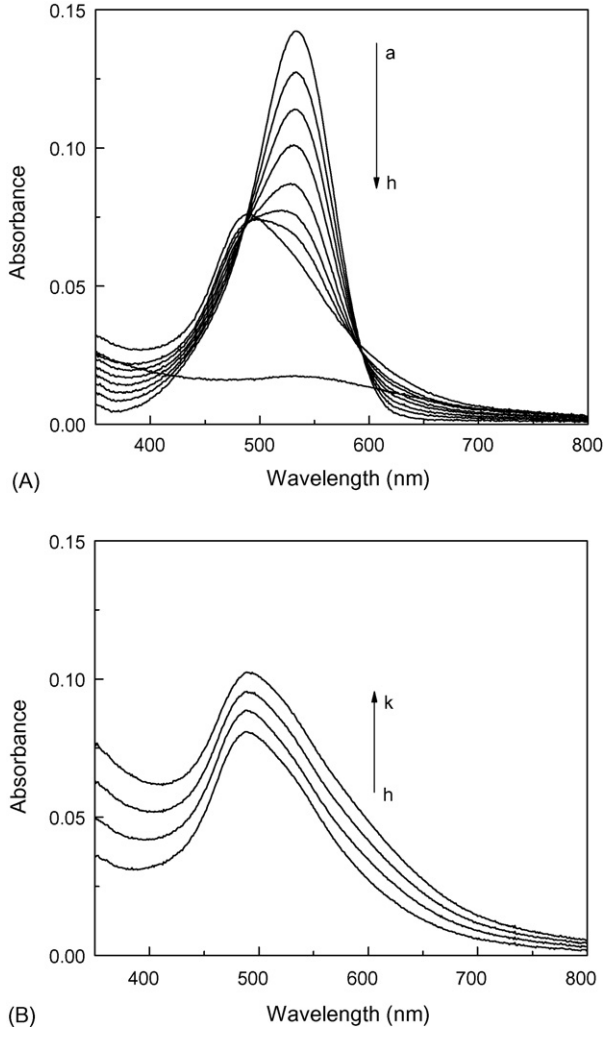

Fig. 2. Absorption spectra of 5×10^{-6} M NR in the presence of various concentrations of MPCs (10^{-6} M): (a) 0; (b) 1.7; (c) 3.3; (d) 5; (e) 6.7; (f) 8.3; (g) 10; (h) 13; (i) 20; (j) 26; (k) 33. Absorption spectrum of free MPCs (1×10^{-5} M) is shown in the lower part of (A).

Fig. 2(A), with the increasing concentration of gold nanoparticles (1.7×10^{-6} M–1.3×10^{-5} M), the absorption intensity of the 534 nm decreases gradually, accompanying with a slight increase of the absorbance in the shorter wavelength. The peak position of 534 nm remains almost unchanged, and two isosbestic points are observed at 488 nm and 594 nm. When the concentration of NR is more than 1.3×10^{-5} M (see Fig. 2(B)), the absorption in the entire visible region increases with the appearance of a peak around 480 nm. The absorption peak at 534 nm gradually merges with the surface plasmon absorption of the gold nanoparticles which is shown in the lower part of Fig. 2(A). In addition, the color of NR solution is bleached to some extent upon the mixing of gold nanoparticles.

The above changes of NR absorption spectrum on the addition of MPCs indicate a strong interaction of NR with MES-MPCs. At pH 6.0, NR molecules are known to mainly exist in the acid form with a positive charge, and the mercaptoethane sulfonate stabilized MPCs prepared in the experiment have abundant negative charges produced by the sulfonic groups. Hence one can expect strong electrostatic interactions between two components in aqueous solution. As a result, NR molecules are closely adsorbed onto the surface of MPCs, which leads to the formation of dye–nanoparticles assembly. The absorption at 534 nm, which is attributed to the acid form of NR, appears to bleach upon adsorption to nanoparticles. This indicates the preference of acid form of NR for the adsorption onto the negatively charged nanoparticles. The appearance of two well-defined isosbestic points when the concentration of NR is less than 1.3×10^{-5} M implies the equilibrium between the free and adsorbed NR molecules, which further verifies the existence of interaction in the solution.

It is very interesting to discuss the spectral changes observed in Fig. 2(B) (increase of the absorption in the entire visible region, and the appearance of an absorption peak around 480 nm) where the concentration of NR is more than 1.3×10^{-5} M. As known, dye molecules tend to form aggregates in aqueous solution, and strong electronic coupling between the molecules in dye aggregates can cause either a blue shift (H-type) or red shift (J-type) of the absorption band [13]. Thus, the appearance of an absorption band in the shorter wavelength in our experiment may arise from the formation of H-aggregation. However, there is also another possibility that can contribute to this absorption band, on considering that the neutral form of NR has intense absorption in this region. In addition, the added gold nanoparticles at this concentration (above 1.3×10^{-5} M) can also make subtle contributions to the absorption changes in the visible region. Thus it is difficult to assess the reason of the above spectral changes from absorption spectra (Fig. 2) directly.

In order to clarify the intrinsic reason for the spectral changes observed, we then adopted the difference spectra method [16,42]. Difference spectra were obtained by subtracting the nanoparticle-only spectrum from the dye–nanoparticle mixture (as shown in Fig. 3). It is important to note here that the absorption spectrum of MPCs actually is also altered on the adsorption of dye, however, the change is rather small compared with that of NR. As can be seen, in the difference spectra, the absorption around the 480 nm does not show any increase on increasing the

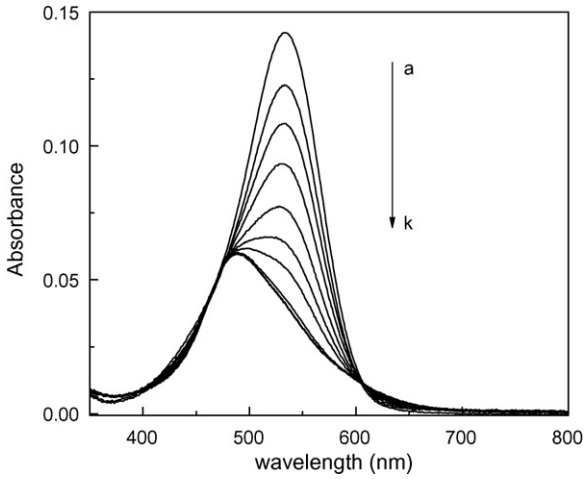

Fig. 3. The obtained difference spectra of Fig. 2 by subtracting the nanoparticle-only spectrum from the dye–nanoparticle mixture. Note curve i–k overlaps each other.

concentration of MPCs. It is evident that the absorption band at 480 nm should originate from the original component existed in the NR solution. On considering the structural equilibrium between the acid form and neutral form in NR aqueous solution at pH 6.0, the absorption peak at 480 nm can then be attributed to the neutral form of NR, which survives after the adsorption onto gold nanoparticles. In addition, the fact that no new absorption band appears on the addition of MPCs also rules out the possibility of forming dye aggregates upon the adsorption of NR on the MPCs. Previous studies have shown that the optical properties of gold nanoparticles also change upon the adsorption of dye, because the position and intensity of the gold surface-plasmon absorption band depends strongly on the optical and electronic properties of the medium surrounding the particles [5,43,44]. However, due to the intense absorption of NR in the wavelength 500–600 nm, the subtle absorption changes of gold nanoparticles are masked. In addition, on the subtraction of MPCs absorption, the resultant spectra remain almost unchanged when the concentration of MPCs is more than 1.3×10^{-5} M. It means that the overall increase we observed in Fig. 2 is just caused by the addition of the gold plasmon absorption. The addition of further amounts of MPCs (more than 1.3×10^{-5} M) to the NR solution actually do not cause any perceptible changes, mainly due to the absorption saturation of NR on MPCs.

3.3. Desorption of NR from MES-MPCs on addition of electrolytes

From the above absorption results, we analyze that electrostatic interaction should be the dominating driving forces for the adsorption of NR onto MPCs. If the formation of NR–MPCs complex is really driven by electrostatic forces, addition of electrolytes to the NR–MPCs complex should result in desorption of NR from the MPCs. Since this complex is formed by cooperative electrostatic forces, due to the introduction of electrolytes, the ionic strength of the medium will be increased which can screen the charges on the assembly [45,46]. As a result, the cooperative association becomes weaker and dissociation of the complex

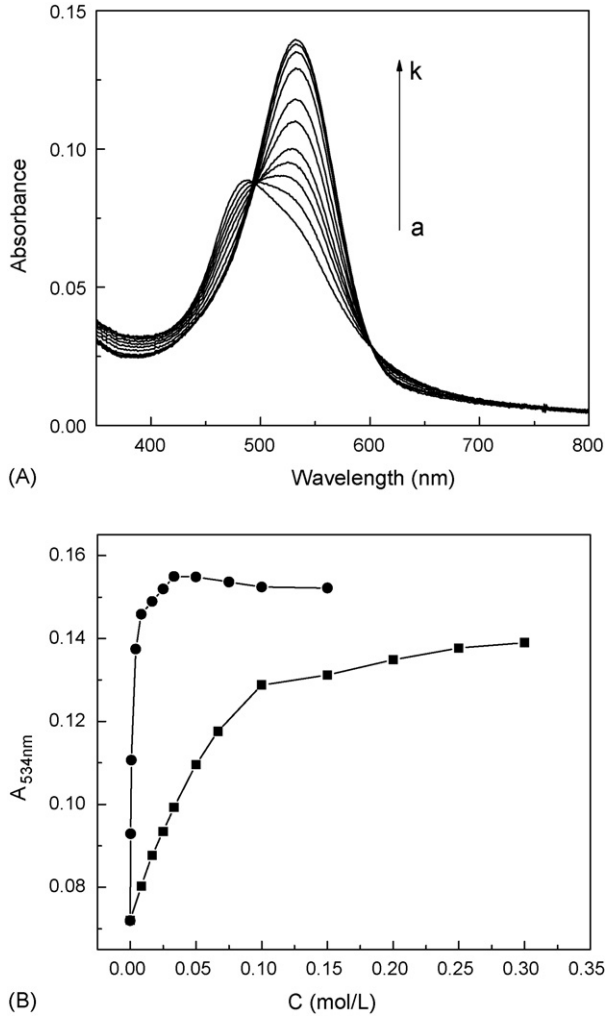

Fig. 4. (A) Absorption spectra of solutions containing 1.3×10^{-5} M MPCs and 5×10^{-6} M NR in the presence of various concentrations of NaCl (M): (a) 0; (b) 0.0083; (c) 0.017; (d) 0.025; (e) 0.033; (f) 0.05; (g) 0.067; (h) 0.1; (i) 0.2; (j) 0.25; (k) 0.3. (B) The absorbance value of the NR–MPCs mixture solutions at 534 nm in the presence of various concentrations of electrolytes: (●) $CaCl_2$ and (■) NaCl.

occurs. It is noteworthy that for the commonly prepared colloids like citrate-protected metal nanoparticles, the addition of electrolytes will result in obvious aggregation of the nanoparticles. However, stemming from the densely packed thiolate layers and the electrostatic repulsion, the as-prepared MES-MPCs can even withstand the saturated NaCl solution without aggregation [31]. This excellent stability of MPCs further allows us to investigate the effect of electrolytes on the NR–MPCs mixture, which is composed of 1.3×10^{-5} M MPCs and 5×10^{-6} M NR.

As shown in Fig. 4(A), with the addition of NaCl into the solution, the absorption in the wavelength 500–600 nm increases gradually and finally develops into a sharp peak at 534 nm, which is the characteristic absorption band of free NR. Also, two well-defined isosbestic points are observed at 492 nm and 600 nm, respectively. The absorption reaches a plateau when the NaCl concentration is up to 0.25 M. The above phenomena indicate that desorption of NR do occur on the addition of electrolytes. This also verifies the electrostatic nature of the

adsorption behavior. Moreover, with the addition of NaCl, the NR solution turns to red in a short time, which also indicates the release of NR from the MPCs. In order to investigate the charge effect on the desorption of NR, we then tested $CaCl_2$, the cation of which is divalent. The experiment shows a similar desorption phenomenon, except that the absorption reaches a plateau at a smaller electrolyte concentration (0.05 M), and the final absorbance is larger than that of NaCl (as shown in Fig. 4(B)). This shows the dication Ca^{2+} is more effective on desorption of NR from the assembly. Electrolyte salts with different anions (Cl^-, NO_3^-) were also investigated, and the results indicated nearly no difference. As a control experiment, we also studied the effect of electrolyte salts on the optical properties of both dye molecules and MPCs individually. The results show that on the addition of these electrolyte salts, the absorption spectra of both components exhibit just slight changes which mainly due to the alteration of the solution refractive index [42,47]. Thus on desorption of the adsorbed dye molecules in the presence of electrolytes, the electrostatic nature of the adsorption is confirmed. Moreover, based on the electrostatic adsorption nature and the excellent stability of MPCs against the electrolytes, we present here a quasi-reversible adsorption/desorption model between nanoparticles and photoactive molecules, which are expected to find potential applications on the design of novel nanodevices for sensing, switching, and drug delivery [5,18].

3.4. Quenching of NR fluorescence on the adsorption of MES-MPCs

Since NR is a fluorescing dye [48], its absorption behavior onto the MPCs can also be characterized by fluorescence spectroscopy. In order to minimize effects of excitation attenuation and solution self-absorption, the experiments presented here use quite dilute solutions. Fig. 5 shows the fluorescence spectra of 2×10^{-6} M NR in the presence of various concentrations of MPCs. Here, NR exhibits an emission maximum at 635 nm when excited at 540 nm in aqueous solutions, at pH 6.0. It can be seen that with increasing the concentration of MPCs, the NR fluorescence intensity decreases distinctly without changing the position of emission maximum. Quenching of the dye fluorescence by the metal nanoparticles that results in energy transfer to the metal particles has been reported earlier [17,20,49,50], and gold nanoparticles are known to exhibit efficient energy transfer behavior as excited state quenchers. So once the NR molecules adsorb onto the MPC surfaces, resonance energy transfer occurs between NR and the MPCs. As a result, the fluorescence of adsorbed NR is quenched. Addition of excess amounts of mercaptoethanesulfonic salt to the NR solution produces no perceptible change of the fluorescence intensity, which further shows that this quenching effect must be attributed to the Au core of the MPCs.

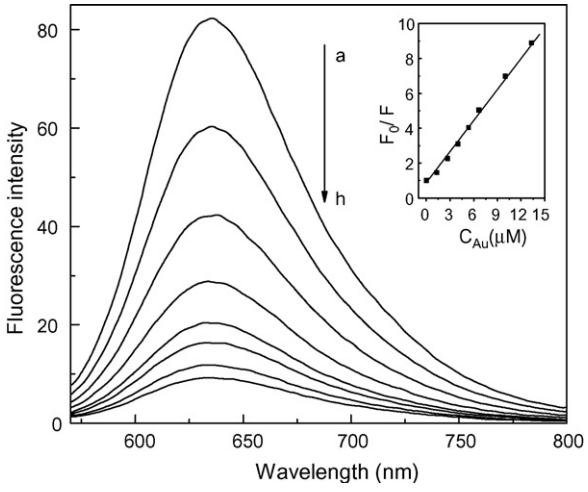

Fig. 5. Fluorescence emission spectra of 2×10^{-6} M NR in the presence of 2.7 nm MPCs at pH 6.0, with the concentration (10^{-6} M): (a) 0; (b) 1.3; (c) 2.7; (d) 4; (e) 5.3; (f) 6.7; (g) 10; (h) 13. Inset: Stern–Volmer plots of NR with the increasing concentrations of MPCs.

Fluorescence intensity data were then analyzed using Stern–Volmer equation [51]:

$$\frac{F_0}{F} = 1 + K_{SV}[Q] \quad (1)$$

where F_0 and F are the fluorescence intensities at 635 nm in the absence and presence of quencher (MPCs), respectively, K_{SV} the Stern–Volmer fluorescence quenching constant, which is a measurement of the efficiency of quenching, and [Q] is the quencher concentration. The inset in Fig. 5 shows the Stern–Volmer plots, F_0/F versus [MPCs], according to Eq. (1). K_{SV}, calculated by linear regression of the plots, was 6.2×10^5 M^{-1}. As known, fluorescence quenching can occur by different mechanisms, which are usually classified as dynamic quenching (collisional quenching) and static quenching (complex formation) [51,52]. In our case, due to the formation of NR–MPCs assembly by the electrostatic adsorption, static quenching is certain to be responsible for the quenching. Then question arises whether dynamic quenching contributes to the quenching of NR fluorescence. Suppose dynamic quenching did contribute to the quenching, we should also observe the decrease of NR fluorescence intensity at which the NR molecules mainly exist in the neutral form. Because the neutral form of NR are not expected to exhibit electrostatic adsorption to MPCs, dynamic quenching should be the only reason responsible for quenching the fluorescence of the neutral form of NR if the quenching did occur. We then choose to perform the quenching experiment at pH 7.8, since at this pH the NR molecules mostly exist in the neutral form. The experiment shows that NR fluorescence is also quenched on the addition of MPCs at pH 7.8, but the quenching constant (K_{SV}) is two orders less than that at pH 6.0 (as shown in Fig. 6). This indicates that dynamic quenching also contributes to the quenching of NR fluorescence on the adsorption onto MPCs. However, the dominating quenching mechanism is static (formation of the dye–MPCs assembly).

To study the size effect of this energy transfer quenching, we then investigated the quenching of NR fluorescence by the MPCs with average diameter of 5.0 nm. As shown in Fig. 7, at the same concentrations of particles as used for the MPCs, the NR fluorescence is quenched to about 12% of its initial value for the 5.0 nm MPCs, while nearly 20% survives for the 2.7 nm MPCs. It is evi-

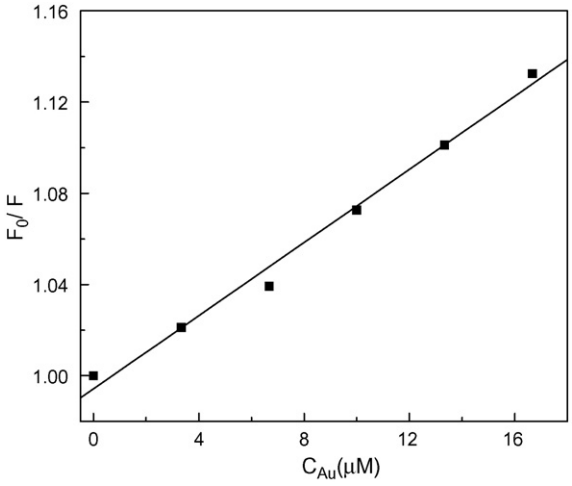

Fig. 6. Stern–Volmer plots of NR (2×10^{-6} M) in the presence of various concentrations of MPCs at pH 7.8. The linear regression gives $K_{SV} = 8.0 \times 10^3$ M^{-1}.

dent that the MPCs quenching is strongly size-dependent, and larger gold particles are efficient quenchers of molecular fluorescence, which agrees with the previous study [28,29]. This size dependent quenching can be rationalized by the physical nature and quantum size effects of metal nanoparticles. As known, quantum size effects originate for gold nanoparticles below 3.2 nm, which results in their transformation from metallic to semiconductor/insulator domain, thus larger gold nanoparticles are metallic in nature and energy transfer mechanism dominates in such systems. As a result, larger particles become efficient quenchers of dye fluorescence than that with smaller core size.

3.5. Quenching release of NR from MES-MPCs on the addition of electrolytes

The above experiments show that on the addition of electrolyte salts, NR molecules will be released from the NR–MPCs

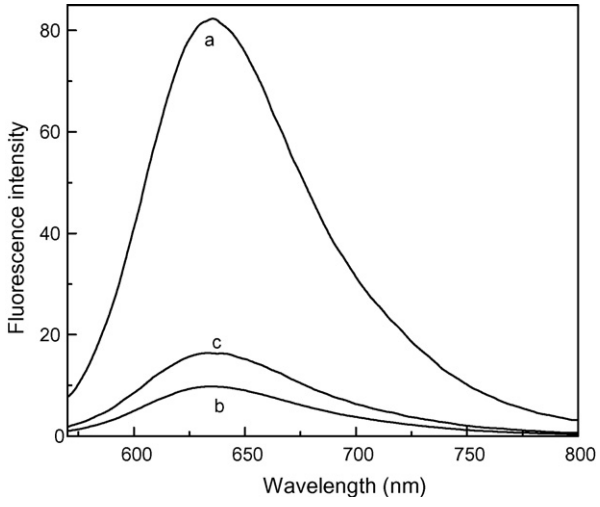

Fig. 7. Fluorescence emission spectra of 2×10^{-6} M NR in the absence (curve a) and presence of 1.1×10^{-8} M gold nanoparticles with average core size of 5.0 nm (curve b) and 2.7 nm (curve c) at pH 6.0.

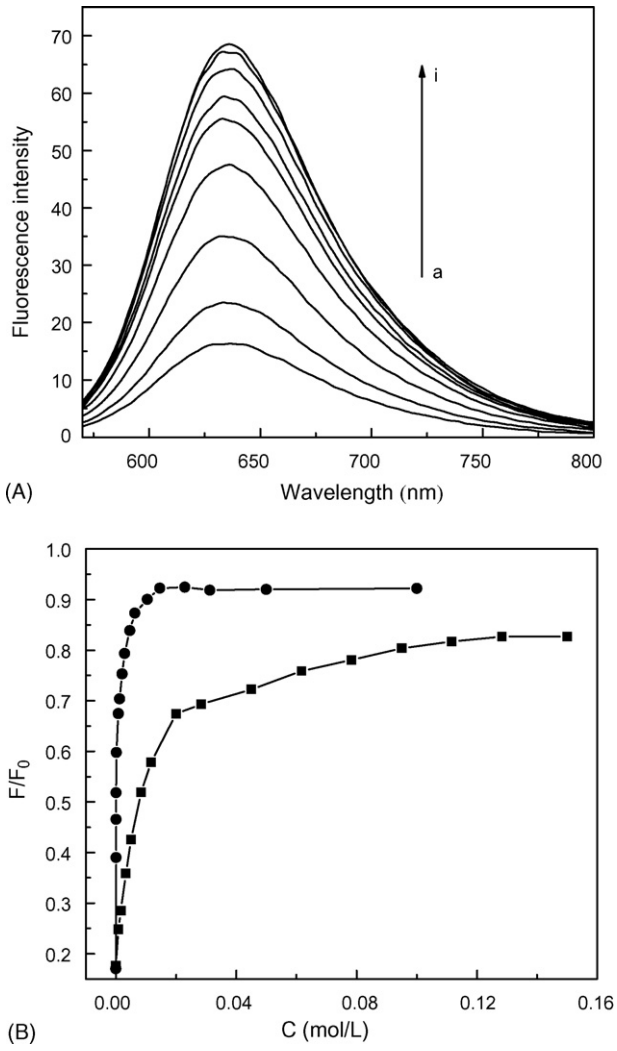

Fig. 8. (A) Fluorescence emission spectra of solutions containing 2×10^{-6} M NR and 6.67×10^{-6} M MPCs in the presence of various concentrations of NaCl (M): (a) 0; (b) 0.0017; (c) 0.005; (d) 0.012; (e) 0.02; (f) 0.045; (g) 0.078; (h) 0.11; (i) 0.15. (B) Relative fluorescence intensity (F/F_0) of the NR–MPCs mixture solutions in the presence of various concentrations of electrolytes: (●) $CaCl_2$ and (■) NaCl.

assembly, which can be monitored by the absorption spectroscopy. Based on the fluorescent property of NR dye, we show that this release process can also be monitored by the fluorescence spectroscopy. As shown in Fig. 8(A), the emission intensity of the NR–MPCs mixture solution (2×10^{-6} M NR and 6.7×10^{-6} M MPCs) increases immediately on the addition of electrolytes (NaCl), which indicates a sharp release of NR into the solution. This recovery of fluorescence on the addition of electrolytes is generally known as quenching release [28]. With increasing the NaCl concentration, finally about 83% of the initial fluorescence is recovered when the NaCl concentration is 0.15 M. Further addition of NaCl causes no perceptible changes on the fluorescence. This further indicates most of the adsorbed NR molecules can be released on the addition of electrolytes. As that in the absorption study, we also investigated the effect of dication Ca^{2+} on the quenching release. Fig. 8(B)

shows the results in terms of F/F_0 (F, F_0 have the same meanings as in Eq. (1)) versus the concentration of electrolyte salts. As shown, the fluorescence intensity reaches its maximum at a relatively smaller concentration 0.02 M compared with Na^+, and nearly 92% of its initial value is recovered at last. The results here accord well with that in the absorption study that the extent of release depends strongly on the specific electrolyte cation, and dication Ca^{2+} is more effective than univalent Na^+ in releasing NR from the assembly. Thus here we present a successful example of investigating the adsorption behavior of photoactive molecules by utilizing the quenching effect of metal nanoparticles. This unique quenching effect between MPCs and adsorbed molecules is also expected to serve as a detector of the extent of kinetic- or equilibrium-controlled binding interactions such as host–guest, antibody–antigen, etc. [53–55].

4. Conclusions

In conclusion, we studied the adsorption behavior of Neutral Red dye on mercaptoethane sulfonate protected gold clusters by UV–vis absorption spectroscopy and fluorescence spectroscopy. NR molecules are closely adsorbed onto the surface of MPCs by the electrostatic attractive interactions. The optical properties of NR molecules are significantly influenced upon the adsorption, and no aggregations form in the adsorption, which is revealed by the difference spectrum method. On addition of electrolytes, NR molecules are found to be released from the NR–MPCs assembly, which is monitored by both absorption and fluorescence spectroscopy. In addition, dication Ca^{2+} is more effective in the release of NR than univalent Na^+. Moreover, on the adsorption of gold nanoparticles, NR fluorescence is significantly quenched. Both static and dynamic quenching mechanisms contribute to the quenching of NR fluorescence, while the former seems to be the dominating factor. Also this energy transfer quenching exhibits strongly dependence of Au core size. It is greatly anticipated that this research will provide further insight into the mechanism behind photoactive molecules–metal nanoparticles interactions, and facilitate the design and fabrication of nanodevices, biosensors.

Acknowledgements

This work is supported by National Natural Science Foundation of China (nos. 20427003, 20575064).

References

[1] Y. Wang, N. Herron, Science 273 (1996) 632–634.
[2] P.V. Kamat, in: P.V. Kamat, D. Meisel (Eds.), Semiconductor Nanoclusters—Physical, Chemical and Catalytic Aspects, Elsevier Science, Amsterdam, 1997, p. 237.
[3] T.K. Sau, A. Pal, T. Pal, J. Phys. Chem. B 105 (2001) 9266–9272.
[4] K. Dick, T. Dhanasekaran, Z. Zhang, D. Meisel, J. Am. Chem. Soc. 124 (2002) 2312–2317.
[5] M.C. Daniel, D. Astruc, Chem. Rev. 104 (2004) 293–346.
[6] R. Shenhar, V.M. Rotello, Acc. Chem. Res. 36 (2003) 549–561.
[7] K.G. Thomas, P.V. Kamat, Acc. Chem. Res. 36 (2003) 888–898.
[8] H. Imahori, H. Norieda, H. Yamada, Y. Nishimura, I. Yamazaki, Y. Sakata, S. Fukuzumi, J. Am. Chem. Soc. 123 (2001) 100–110.
[9] A. Hagfeldt, M. Gratzel, Chem. Rev. 95 (1995) 49–68.
[10] A. Dawson, P.V. Kamat, J. Phys. Chem. B 104 (2000) 11842–11846.
[11] G. Ramakrishna, D.A. Jose, D.K. Kumar, A. Das, D.K. Palit, H.N. Ghosh, J. Phys. Chem. B 109 (2005) 15445–15453.
[12] C. Pagba, G. Zordan, E. Galoppini, E.L. Piatnitski, S. Hore, K. Deshayes, P. Piotrowiak, J. Am. Chem. Soc. 126 (2004) 9888–9889.
[13] C. Nasr, D. Liu, S. Hotchandani, P.V. Kamat, J. Phys. Chem. 100 (1996) 11054–11061.
[14] R.L. Sherman, W.T. Ford, Langmuir 21 (2005) 5218–5222.
[15] H. Tu, D.F. Kelley, Nano Lett. 6 (2006) 116–122.
[16] S. Franzen, J.C.W. Folmer, W.R. Glommm, R. O'Neal, J. Phys. Chem. A 106 (2002) 6533–6540.
[17] E. Dulkeith, A.C. Morteani, T. Niedereichholz, T.A. Klar, J. Feldmann, Phys. Rev. Lett. 89 (2002) 203002-1–1203002-4.
[18] S.J. Chen, H.T. Chang, Anal. Chem. 76 (2004) 3727–3734.
[19] S.K. Ghosh, A. Pal, S. Kundu, S. Nath, T. Pal, Chem. Phys. Lett. 395 (2004) 366–372.
[20] Y. Ding, X. Zhang, X. Liu, R. Guo, Langmuir 22 (2006) 2292–2298.
[21] M. Brust, J. Fink, D. Bethell, D.J. Schiffrin, C.J. Kiely, J. Chem. Soc., Chem. Commun. (1995) 1655–1656.
[22] A.C. Templeton, W.P. Wuelfing, R.W. Murray, Acc. Chem. Res. 33 (2000) 27–36.
[23] G. Wang, T. Huang, R.W. Murray, L. Menard, R.G. Nuzzo, J. Am. Chem. Soc. 127 (2005) 812–813.
[24] G. Wang, J. Zhang, R.W. Murray, Anal. Chem. 74 (2002) 4320–4327.
[25] H. Imahori, S. Fukuzumi, Adv. Mater. 13 (2001) 1197–1199.
[26] T. Gu, J.K. Whitesell, M.A. Fox, Chem. Mater. 15 (2003) 1358–1366.
[27] A. Aguila, R.W. Murray, Langmuir 16 (2000) 5949–5954.
[28] T. Huang, R.W. Murry, Langmuir 18 (2002) 7077–7081.
[29] P.P.H. Cheng, D. Silvester, G. Wang, G. Kalyuzhny, A. Douglas, R.W. Murray, J. Phys. Chem. B 110 (2006) 4637–4644.
[30] B.I. Ipe, S. Mahima, K.G. Thomas, J. Am. Chem. Soc. 125 (2003) 7174–7175.
[31] X. Zou, H. Bao, H. Guo, L. Zhang, L. Qi, J. Jiang, L. Niu, S. Dong, J. Colloid Interf. Sci. 295 (2005) 401–408.
[32] J.C. Lumanna, K.A. McCracken, Anal. Biochem. 142 (1984) 117–125.
[33] M. Haumann, W. Junge, Biochemistry 33 (1994) 864–872.
[34] C. Sousa, T.S. Melo, M. Gèze, J. Gaullier, J. Mazière, R. Santus, Photochem. Photobiol. 63 (1996) 601–607.
[35] R. Osborne, M.A. Perkins, Food Chem. Toxicol. 32 (1994) 133–142.
[36] G. Chen, C.L. Hanson, T.J. Ebner, J. Neurophysiol. 76 (1996) 4169–4174.
[37] K.W. Woodburn, N.J. Vardaxis, J.S. Hill, A.H. Kaye, D.R. Phillips, Photochem. Photobiol. 54 (1991) 725–732.
[38] J.P. Choi, A.J. Bard, J. Electroanal. Chem. 573 (2004) 215–225.
[39] F.G. Walz Jr., B. Terenna, D. Rolince, Biopolymers 14 (1975) 825–837.
[40] J. Jurasova, V. Kuban, Collection Czechoslovak Chem. Commun. 52 (1987) 2401–2411.
[41] X. Jiang, L. Shang, Z. Wang, S. Dong, Biophys. Chem. 118 (2005) 42–50.
[42] K.G. Thomas, J. Zajicek, P.V. Kamat, Langmuir 18 (2002) 3722–3727.
[43] O.V. Makarova, A.E. Ostafin, H. Miyoshi, J.R. Norris, J.D. Meisel, J. Phys. Chem. B 103 (1999) 9080–9084.
[44] K.G. Thomas, P.V. Kamat, J. Am. Chem. Soc. 122 (2000) 2655–2656.
[45] Y. Zhou, Y. Li, Biophys. Chem. 107 (2004) 273–281.
[46] T. Reschel, C. Konak, D. Oupicky, L.W. Seymour, K. Ulbrich, J. Control. Rel. 81 (2002) 201–217.
[47] P. Mulvaney, Langmuir 12 (1996) 788–800.
[48] M.C. Singh, H. Pal, A.C. Bhasikuttan, A.V. Sapre, Photochem. Photobiol. 69 (1999) 529–535.
[49] C. Fan, S. Wang, J.W. Hong, G.C. Bazan, K.W. Plaxco, A.J. Heeger, PNAS 100 (2003) 6297–6301.

[50] B.I. Ipe, K.G. Thomas, S. Barazzouk, S. Hotchandani, P.V. Kamat, J. Phys. Chem. B 106 (2002) 18–21.
[51] J.R. Lakowicz, Principles of Fluorescence Spectroscopy, Kluwer Academic/Plenum Press, New York, 1999.
[52] J. Kang, Y. Liu, M. Xie, S. Li, M. Jiang, Y. Wang, Biochim. Biophys. Acta 1674 (2004) 205–214.
[53] C.M. Niemeyer, Angew. Chem. Int. Ed. 40 (2001) 4128–4158.
[54] R. Hong, G. Han, J.M. Fernandez, B. Kim, N.S. Forbes, V.M. Rotello, J. Am. Chem. Soc. 128 (2006) 1078–1079.
[55] L. Ao, F. Gao, B. Pan, R. He, D. Cui, Anal. Chem. 78 (2006) 1104–1106.